

Spectroscopy and molecule opacity investigation on excited states of SiS

Rui Li(李瑞), Haonan Lv(吕浩男), Jiqun Sang(桑纪群), Xiaohua Liu(刘晓华), Guiying Liang(梁桂颖), and Yong Wu(吴勇)

Citation: Chin. Phys. B, 2024, 33 (**5**): 053101. DOI: 10.1088/1674-1056/ad20dc
Journal homepage: http://cpb.iphy.ac.cn; http://iopscience.iop.org/cpb

What follows is a list of articles you may be interested in

Microscopic mechanism of plasmon-mediated photocatalytic H_2 splitting on Ag-Au alloy chain

Yuhui Song(宋玉慧), Yirui Lu(芦一瑞), Axin Guo(郭阿鑫), Yifei Cao(曹逸飞), Jinping Li(李金萍), Zhengkun Fu(付正坤), Lei Yan(严蕾), and Zhenglong Zhang(张正龙)
Chin. Phys. B, 2024, 33 (**3**): 033101. DOI: 10.1088/1674-1056/ad123d

Mutual neutralization in low-energy collisions of $Na^+ + H^-$ ions

Kun Wang(王堃), Chuan Dong(董川), Yizhi Qu(屈一至), Yong Wu(吴勇), Xiaohe Lin(林晓贺), and Robert J. Buenker
Chin. Phys. B, 2023, 32 (**8**): 083103. DOI: 10.1088/1674-1056/acd624

Ridge regression energy levels calculation of neutral ytterbium (Z = 70)

Yushu Yu(余雨姝), Chen Yang(杨晨), and Gang Jiang(蒋刚)
Chin. Phys. B, 2023, 32 (**3**): 033101. DOI: 10.1088/1674-1056/acac08

Molecule opacity study on low-lying states of CS

Rui Li(李瑞), Jiqun Sang(桑纪群), Xiaohe Lin(林晓贺), Jianjun Li(李建军), Guiying Liang(梁桂颖), and Yong Wu(吴勇)
Chin. Phys. B, 2022, 31 (**10**): 103101. DOI: 10.1088/1674-1056/ac834f

Molecule opacities of $X^2\Sigma^+$, $A^2\Pi$, and $B^2\Sigma^+$ states of CS^+

Xiao-He Lin(林晓贺), Gui-Ying Liang(梁桂颖), Jian-Guo Wang(王建国), Yi-Geng Peng(彭裔耕), Bin Shao(邵彬), Rui Li(李瑞), Yong Wu(吴勇)
Chin. Phys. B, 2019, 28 (**5**): 053101. DOI: 10.1088/1674-1056/28/5/053101

Spectroscopy and molecule opacity investigation on excited states of SiS

Rui Li(李瑞)[1,2], Haonan Lv(吕浩男)[3], Jiqun Sang(桑纪群)[3], Xiaohua Liu(刘晓华)[3], Guiying Liang(梁桂颖)[4,2], and Yong Wu(吴勇)[2,5,†]

[1] *College of Teacher Education, Qiqihar University, Qiqihar* 161006, *China*
[2] *National Key Laboratory of Computational Physics, Institute of Applied Physics and Computational Mathematics, Beijing* 100088, *China*
[3] *Department of Physics, College of Science, Qiqihar University, Qiqihar* 161006, *China*
[4] *School of Data Science and Artificial Intelligence, Jilin Engineering Normal University, Changchun* 130052, *China*
[5] *HEDPS, Center for Applied Physics and Technology, Peking University, Beijing* 100084, *China*

(Received 30 November 2023; revised manuscript received 10 January 2024; accepted manuscript online 22 January 2024)

The SiS molecule, which plays a significant role in space, has attracted a great deal of attention for many years. Due to complex interactions among its low-lying electronic states, precise information regarding the molecular structure of SiS is limited. To obtain accurate information about the structure of its excited states, the high-precision multireference configuration interaction (MRCI) method has been utilized. This method is used to calculate the potential energy curves (PECs) of the 18 Λ–S states corresponding to the lowest dissociation limit of SiS. The core–valence correlation effect, Davidson's correction and the scalar relativistic effect are also included to guarantee the precision of the MRCI calculation. Based on the calculated PECs, the spectroscopic constants of quasi-bound and bound electronic states are calculated and they are in accordance with previous experimental results. The transition dipole moments (TDMs) and dipole moments (DMs) are determined by the MRCI method. In addition, the abrupt variations of the DMs for the $1^5\Sigma^+$ and $2^5\Sigma^+$ states at the avoided crossing point are attributed to the variation of the electronic configuration. The opacity of SiS at a pressure of 100 atms is presented across a series of temperatures. With increasing temperature, the expanding population of excited states blurs the band boundaries.

Keywords: SiS, opacity, excited state, spectroscopic constant, configuration interaction

PACS: 31.15.aj, 31.50.Df, 31.15.ag **DOI:** 10.1088/1674-1056/ad20dc

1. Introduction

The SiS molecule plays a significant role in space, which has attracted a great of interest from study groups.[1] The molecule has been observed in the microwave region through emission from the carbon star IRC+10216 molecular envelope. The molecule has also been found in cool S stars,[2,3] oxygen-rich stars[4] and the interstellar medium.[5] It is thought that SiS molecules are formed through pathways of Si+SO and Si+SO_2 in space; however, the destruction reaction is considered as SiS+O.[6] Due to its astronomical importance, the molecular structure, spectroscopy and opacity of the SiS molecule have been studied in previous investigations.

Pioneering experimental studies on the vibronic emission of $A^1\Pi$–$X^1\Sigma^+$ of SiS were carried out by Barrow and Jevons.[7] Since then, several experimental studies have focused on the spin-allowed transitions $E^1\Sigma^+$–$X^1\Sigma^+$, $D^1\Pi$–$X^1\Sigma^+$ and $A^1\Pi$–$X^1\Sigma^+$. A series of ultraviolet bands were photographed by Vago and Barrow,[8] and vibrational analyses were carried out to obtain the vibrational constants of $E^1\Sigma^+$ and $D^1\Pi$. Nair[9] obtained the dissociation energy (D_e) and experimental potential-energy curves (PECs) by employing the Rydberg–Klein–Rees method. Later, Gopal *et al.*[10] recorded the isotope shift phenomenon for $^{28}Si^{32}S$ and $^{28}Si^{34}S$ in the visible and UV regions, confirming the vibrational assignments of $D^1\Pi$–$X^1\Sigma^+$ in the 260 nm–390 nm region. Sunanda *et al.*[11] obtained the Franck–Condon factors (FCFs) from the observed $E^1\Sigma^+$–$X^1\Sigma^+$ band system. Recently, rotational lines generated by high-vibrational levels of SiS[12] were observed by employing the Atacama large millimeter array radio telescope, and transitions for isotopologues in high vibrational states were also detected.

From a theoretical point of view, the molecular structures of several excited states of SiS have been studied via different theoretical methods. Robbe *et al.*[13] used self-consistent field configuration interaction (CI) to compute the PECs of the excited states of SiS and determined the primary electronic configuration and spectroscopic constants of several bound states. Chattopadhyaya *et al.*[14] evaluated the electronic spectrum of SiS by utilizing the multireference singles and doubles configuration interaction approach, and studied the spectroscopic properties of $E^1\Sigma^+$–$X^1\Sigma^+$ and $A^1\Pi$–$X^1\Sigma^+$ transitions. Li *et al.*[15] utilized the high-precision multireference configuration interaction (MRCI) approach to compute the 18 Λ–S states of the lowest dissociation limit of SiS and discussed the transition properties of $A^1\Pi$ and $E^1\Sigma^+$ states. Upadhyay *et al.*[1] utilized the experimental PECs and the theoretical dipole moment (DM) curves to determine the rotation−vibrational line lists of the ground state of SiS. More recently, vibrational constants and analytical potential energy functions[16] were obtained by employing the variational algebraic method.

†Corresponding author. E-mail: wu_yong@iapcm.ac.cn

© 2024 Chinese Physical Society and IOP Publishing Ltd

As discussed above, the spectroscopic properties and electronic structures of the SiS molecule have been investigated by a series of research groups. However, the major focus in previous theoretical computations of the SiS molecule has been on the structures of several low-lying excited states. Owing to the large state density of the excited states, information about the high-precision structure of the excited states of SiS is still limited. Previous work mainly focused on the electronic structures of singlet states $X^1\Sigma^+$, $A^1\Pi$, $D^1\Pi$ and $E^1\Sigma^+$. The electronic configuration of the low-lying Λ–S states of SiS has not been extensively investigated. The variation of DMs in the avoided crossing region has not been studied. To the best of our knowledge, the only rotation–vibrational line lists for the ground state $X^1\Sigma^+$ were generated by Upadhyay *et al.*[1] Simulated spectra of the excited states of SiS remain sparse. In this paper, high-precision structures of the excited states of SiS are computed using the MRCI method. The DMs and transition dipole moments (TDMs) from the excited state to the ground state are given by the MRCI level. The variation of DMs in the avoided crossing region is explained by the change in electronic configurations. Finally, the opacity of SiS originating from vibration–rotation transitions at different temperature conditions is evaluated.

2. Theoretical method

In this work, the electronic structures of 18 Λ–S states of the lowest dissociation limit (Si^3P_g+S^3P_g) of SiS are investigated using MOLPRO package.[17] Owing to the limitations of that package, all the calculations in this work were done in the C_{2v} Abelian group. In our calculations, aug-cc-pwCV5Z-DK basis sets[18,19] are adopted to depict Si and S. In the calculation process, the singlet configuration wavefunction of the $X^1\Sigma^+$ of SiS is determined by the Hartree–Fock (HF) method in the bond length range of 1.6–5.0 Å. To consider static correlation effects, multi-configuration wavefunctions are calculated using the complete active space self-consistent field (CASSCF) method[20,21] by employing wavefunctions determined by the HF method as an initial guess. Finally, the eigenenergies of the 18 Λ–S states are calculated with the MRCI approach[22,23] using the CASSCF wavefunctions as a reference. In addition, the Davidson correction[24] is included to overcome the size-consistency error in the MRCI calculation. The active space in the CASSCF calculations is composed of $4a_1$, $2b_1$ and $2b_2$ molecular orbitals, corresponding to Si 3s3p and S 3s3p valence electron orbitals. The core–valence correlation (CV) effect is also considered in the MRCI calculation, and the electrons in 2s2p shells of S and 2s2p shells of Si are correlated; however, the electrons in the 1s inner shell of S and Si are frozen. In addition, the scalar relativistic correction[25,26] is obtained from third-order Douglas–Kroll and Hess integrals.

The electronic Schrödinger equation of SiS can be represented as

$$\hat{H}_e \Psi_e(r,R) = E_e(R)\Psi_e(r,R), \tag{1}$$

where $\hat{H}_e$ is Hamiltonian of the molecules and $\Psi_e(r,R)$ and $E_e(R)$ are the eigenfunction and eigenenergy, respectively. $\hat{H}_e$ is given by the following formula:

$$\hat{H}_e = \sum_{i=1}^{N}\left(-\frac{1}{2}\nabla_i^2\right) + \sum_{i=1}^{N}\left(-\frac{Z_a}{r_{ai}} - \frac{Z_b}{r_{bi}}\right) + \sum_{i<j=1}^{N}\left(\frac{1}{r_{ij}}\right) + \frac{Z_a Z_b}{R}, \tag{2}$$

in which Z_a and Z_b are the nuclear charge numbers of the Si and S atoms.

Based on the eigenenergies in Eq. (1), the eigenvalues of the vibration–rotation states are determined as solutions to the radical Schrödinger equation

$$\left[-\frac{1}{2\mu}\frac{\mathrm{d}^2}{\mathrm{d}R^2} + E_e(R)\right]\chi_{vJ}(R) = E_{vJ}\chi_{vJ}(R), \tag{3}$$

where $E_{vJ}(R)$ is eigenenergy of the vibration–rotation level.

$$A_{v'j',v''j''} = \frac{4}{3}\omega^3_{v'j',v''j''}\alpha^3\frac{S_{J'J''}}{2J''+1} \tag{4}$$

in which

$$S_{J'J''} = |\langle\chi_{v'J'}|D(R)|\chi_{v''J''}\rangle|^2\varphi_{J'J''}, \tag{5}$$

where v' is the vibrational quantum number, J' is the rotational quantum number, α is the fine-structure constant, $\omega_{v'j',v''j''}$ is the transition frequency of different vibration–rotation states, $S_{J'J''}$ is the line strength, $D(R)$ is the TDM and $\varphi_{J',J''}$ is the Hönl–London factor.

On the basis of line strength, the molecular opacity is determined by

$$\sigma = \frac{1}{8\pi(\Delta E''/hc)^2} \times \frac{A(2J'+1)[1-\exp(-\Delta E''/kT]\exp(-E_{V'J',00}hc/kT)}{Q}, \tag{6}$$

where $\Delta E''$ is energy difference between the related two states, c is the speed of light, A is acquired from Eq. (4), k is Boltzmann's constant, $E_{V'J',00}$ is the excitation energy and h is Plank's constant. The partition function $Q(T)$ is determined using the following formula:

$$Q = \sum_{i=1}^{n} Q_{ei}Q_{vi}Q_{ri}\exp\left(-\frac{T_i hc}{kT}\right) \tag{7}$$

in which T_i is the transition energy of i-th electronic state and T is the surrounding temperature.

Based on the calculated vibrational level and vibrational wavefunction, the oscillator strengths $f_{v'v''}$ (in a.u.) is given by the following formula:

$$f_{v'v''} = \frac{2}{3}\times\Delta E\times \mathrm{TDM}^2\times q_{v'v''}, \tag{8}$$

where ΔE is the energy gap between vibrational levels v' and v'', TDM (in units of a.u.) is the average transition DM, and $q_{v'v''}$ is the FCF.

3. Result and discussion

3.1. Electronic structure and spectroscopy

The 18 Λ–S electronic states of the lowest dissociation limit (Si^3P_g+S^3P_g) of the SiS molecules are evaluated at the aug-cc-pwCV5Z-DK/MRCI+Q level of theory. Figure 1 displays an overview of the PECs of those 18 states. To observe the position of the electronic states clearly, the PECs of singlet, triplet and quintet states are listed separately in Figs. 1(a), 1(b) and 1(c). On the basis of the calculated PECs, a series of spectroscopic constants including vibrational frequencies ω_e, anharmonic terms $\omega_e x_e$, adiabatic excitation energy T_e, dissociation energy D_e, equilibrium constant B_e and equilibrium internuclear distance R_e are evaluated, which are provided Table 1.

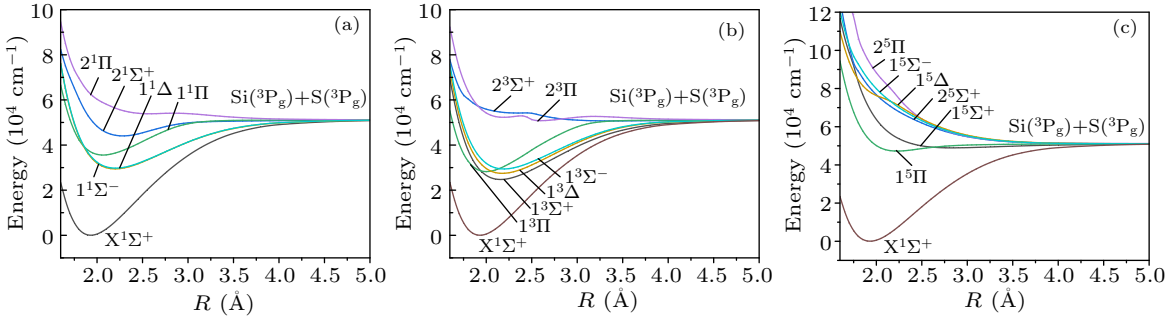


Fig. 1. MRCI+Q potential energy curves for the lowest dissociation limit of SiS.

Table 1. Spectroscopic constants of bound Λ–S states of SiS.

Λ–S stste		T_e (cm^{-1})	ω_e (cm^{-1})	$\omega_e x_e$ (cm^{-1})	B_e (cm^{-1})	R_e (Å)	D_e (cm^{-1})
$X^1\Sigma^+$	This work	0	749.54	2.3923	0.3035	1.9294	50828
	Expt[a]	0	749.64	2.5770	0.303528	1.9293	51619
	Expt[b]	0	749.645	2.58623	0.303528	1.9293	
	Calc[c]	0	733			1.9570	
	Calc[d]					1.9319	
$2^1\Sigma^+$	This work	43230	423	1.9024	0.2223	2.2546	8253
	Expt[e]	41915.8	405.6	1.60	0.22137	2.2591	
	Calc[c]	41383	418			2.2860	
$1^1\Pi$	This work	35589	520	2.5997	0.2654	2.0633	15552
	Expt[e]	35026.84	513.17	2.94	0.26637	2.0595	
	Calc[c]	35385	485			2.1120	
$1^1\Sigma^-$	This work	29463	470	1.7305	0.2342	2.1964	21567
	Expt[e]	28972.8	472.33	2.11	0.2341	2.1970	
	Calc[c]	28235	467			2.2540	
$1^1\Delta$	This work	29787	464	1.7232	0.2331	2.2014	21271
	Expt[e]	29349.2	465.84	2.02	0.2340	2.1970	
	Calc[c]	28532	445			2.2620	
$1^3\Sigma^+$	This work	24747	508	2.0062	0.2428	2.1569	26169
	Expt[f]	24572±10	506±4	2.3±2			
	Calc[c]	23518	504			2.1950	
$1^3\Pi$	This work	28228	612	3.4354	0.2831	1.9976	22926
	Expt[e]	27407.9	624.3	3.97			
	Calc[c]	27378	604			2.0260	
$1^3\Delta$	This work	27478	492	1.7785	0.2390	2.1741	23562
	Expt[e]	27268	484.51	1.89	0.2401	2.1690	
	Calc[c]	26502	480			2.2200	
$1^3\Sigma^-$	This work	29430	473	1.6971	0.2350	2.1927	21668
	Expt[e]	29112.1	469.51	1.94	0.2351	2.1920	
	Calc[c]	28420	462			2.2420	
$1^5\Pi$	This work	47286	402	10.4919	0.2280	2.2257	3836
	Calc[c]	44870	283			2.3420	

[a]Ref. [28], [b]Ref. [27], [c]Ref. [14], [d]Ref. [31], [e]Ref. [29], [f]Ref. [32].

Figures 1(a) and 1(b) clearly show that $2^1\Pi$, $2^3\Pi$ and $2^3\Sigma^+$ are quasi-bound states, while the other nine electronic states are bound states. In Fig. 1(c), the $1^5\Pi$ state is a weakly bound state, which can only hold 21 vibrational energy levels, while the other five quintet states ($1^5\Sigma^+$, $2^5\Sigma^+$, $1^5\Sigma^-$, $2^5\Pi$ and $1^5\Delta$) are repulsive states. The ground state of SiS has $^1\Sigma^+$ symmetry, which is mainly described by a $7\sigma^2 8\sigma^2 3\pi^4 9\sigma^2$ configuration. The ω_e, $\omega_e x_e$, B_e and R_e are evaluated to be 749.54, 2.3923, 0.3035 cm^{-1} and 1.9294 Å, and the deviation between our calculated results and previous experimental data[27] is 0.105, 0.19393, 0.000028 cm^{-1} and 0.0001 Å. The calculated D_e is 50828 cm^{-1}, which is only underestimated by 791 cm^{-1} as compared with the experimental value of 51619 cm^{-1}.[28] The first excited state is $1^3\Sigma^+$, which is mainly described by a $7\sigma^2 8\sigma^2 3\pi^3 9\sigma^2 4\pi^1$ configuration corresponding to $3\pi \rightarrow 4\pi$ excitation relative to that of the $X^1\Sigma^+$. The T_e, ω_e and $\omega_e x_e$ are computed to be 24747, 508 and 2.0062 cm^{-1}, which are consistent with the experimental data[32] of 24572, 506 and 2.3 cm^{-1}. Our calculated R_e of $1^3\Sigma^+$ is 2.1569 Å, which is 0.0381 Å smaller than the configuration interaction result of 2.1950 Å.[14] For the $1^1\Pi$, the electronic configuration is mainly made up of $7\sigma^2 8\sigma^2 3\pi^4 9\sigma^1 4\pi^1$, which associates with the $9\sigma \rightarrow 4\pi$ excitation relative to that of the $X^1\Sigma^+$. Our calculated values of T_e, ω_e and R_e are 35589, 520 cm^{-1} and 2.0633 Å, which are only 562.16, 6.83 cm^{-1} and 0.0038 Å larger than the previous experimental results.[29] The calculated values of $\omega_e x_e$ (2.5997 cm^{-1}) and B_e (0.2654 cm^{-1}) are only 0.3403 cm^{-1} and 0.00097 cm^{-1} smaller than the previous experimental values.[29]

Table 2. Dominant configuration at $R = 1.95$ Å of bound state of SiS.

Λ–S states	Main configuration at $R = 1.95$ Å (%)
$X^1\Sigma^+$	$7\sigma^2 8\sigma^2 3\pi^4 9\sigma^2$ (83.73)
$2^1\Sigma^+$	$7\sigma^2 8\sigma^2 3\pi^3 9\sigma^2 4\pi^1$ (57.61)
	$7\sigma^2 8\sigma^2 3\pi^4 9\sigma^1 10\sigma^1$ (20.9)
$1^1\Pi$	$7\sigma^2 8\sigma^2 3\pi^4 9\sigma^1 4\pi^1$ (78.77)
$1^1\Sigma^-$	$7\sigma^2 8\sigma^2 3\pi^3 9\sigma^2 4\pi^1$ (94.56)
$1^1\Delta$	$7\sigma^2 8\sigma^2 3\pi^3 9\sigma^2 4\pi^1$ (95.58)
$1^3\Sigma^+$	$7\sigma^2 8\sigma^2 3\pi^3 9\sigma^2 4\pi^1$ (95.82)
$1^3\Pi$	$7\sigma^2 8\sigma^2 3\pi^4 9\sigma^1 4\pi^1$ (84.13)
$1^3\Delta$	$7\sigma^2 8\sigma^2 3\pi^3 9\sigma^2 4\pi^1$ (96.09)
$1^3\Sigma^-$	$7\sigma^2 8\sigma^2 3\pi^3 9\sigma^2 4\pi^1$ (94.7)
$1^5\Pi$	$7\sigma^2 8\sigma^2 3\pi^3 9\sigma^1 4\pi^2$ (95.27)

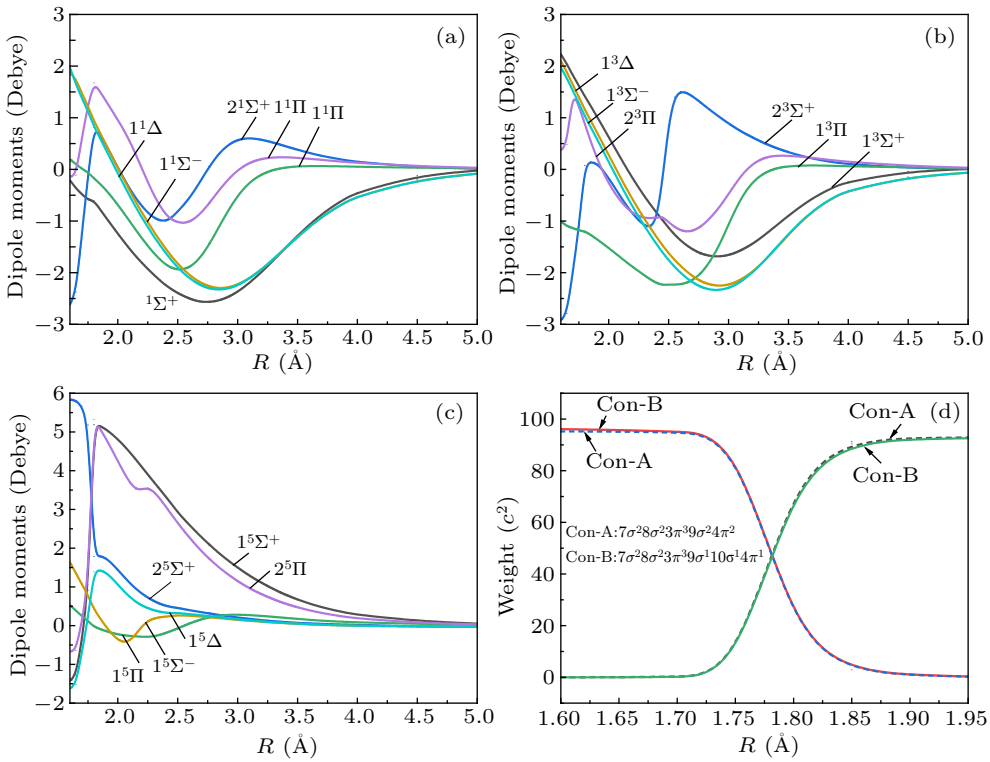


Fig. 2. Dipole moment curves and electronic configuration of the same symmetry state ($1^5\Sigma^+$ and $2^5\Sigma^+$) of SiS.

In order to illustrate the precision of our calculation, the vibrational levels of the $X^1\Sigma^+$, $1^1\Pi$ and $2^1\Sigma^+$ states are provided in the supplementary material (Tables S1–S3). The previously available experimental and theoretical results are also listed in Tables S1–S3. As displayed in the supplementary material, our calculated vibrational levels of the $X^1\Sigma^+$, $1^1\Pi$ and $2^1\Sigma^+$ states are in good agreement with both the experimental values and the existing theoretical results. For the excited states $1^1\Pi$ and $2^1\Sigma^+$, the maximum deviation is 1.9% and 2.5%, respectively.

As is well known, DMs and TDMs play a crucial role in the bonding properties and transition characteristics of molecules. The DMs of 18 Λ–S states of the SiS molecule are obtained by the aug-cc-pwCV5Z-DK/MRCI level of theory.

For clarity, the DM curves corresponding to the singlet, triplet and quintuplet states are provided, respectively, in Figs. 2(a)–2(c). The variations of electronic configuration along with internuclear distance for $1^5\Sigma^+$ and $2^5\Sigma^+$ states are displayed in Fig. 2(d). The TDM values of $2^1\Sigma^+$–$X^1\Sigma^+$ and $1^1\Pi$–$X^1\Sigma^+$ transitions are determined at the MRCI level, and the variations of TDMs along with internuclear distance are given in Fig. 3.

As displayed in Fig. 2, the calculated value of the $X^1\Sigma^+$ at an internuclear distance is 1.45 Debye, which is in accordance with the experimental value of 1.74 Debye.[30] Due to the similar bond lengths and dominant electronic configurations of $1^1\Pi$ and $1^3\Pi$, the variation of the DM curve of $1^3\Pi$ is analogous to that of $1^1\Pi$. It can be seen from Fig. 1(c) that the PECs of $1^5\Sigma^+$ and $2^5\Sigma^+$ exhibit an avoided crossing phenomenon near R =1.75 Å. Similarly, we can find that the DM curves of $1^5\Sigma^+$ and $2^5\Sigma^+$ also vary sharply at the avoided crossing point. In order to explain the avoided crossing of the same symmetry, the weights c^2 of the dominant electronic configurations of $1^5\Sigma^+$ and $2^5\Sigma^+$ at a series of internuclear distances are displayed in Fig. 2(d). At $R < 1.75$ Å, the electronic configurations of the $1^5\Sigma^+$ and $2^5\Sigma^+$ states are mainly composed of $7\sigma^2 8\sigma^2 3\pi^2 9\sigma^2 4\pi^2$ (Con-A) and $7\sigma^2 8\sigma^2 3\pi^3 9\sigma^1 10\sigma^1 4\pi^1$ (Con-B), respectively. When the internuclear distance is close to 1.75 Å, the dominant electronic configurations of the $1^5\Sigma^+$ and $2^5\Sigma^+$ states exhibit a sharp change, which also leads to a polarity reversal of the DMs of the two states. At $R > 1.75$ Å, the dominant electron configurations of the $1^5\Sigma^+$ and $2^5\Sigma^+$ states change to $7\sigma^2 8\sigma^2 3\pi^3 9\sigma^1 10\sigma^1 4\pi^1$ and $7\sigma^2 8\sigma^2 3\pi^2 9\sigma^2 4\pi^2$, respectively. At the avoided crossing region, the changes of DM curves for $1^5\Sigma^+$ and $2^5\Sigma^+$ states present a complementary trend, resulting from the exchange of dominant electronic configurations for the two states.

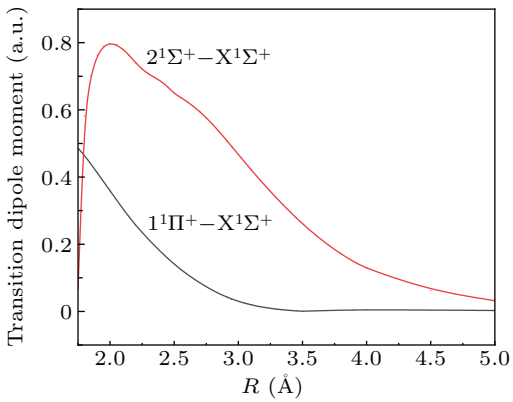


Fig. 3. Transition dipole moment curves for spin-allowed transition $2^1\Sigma^+$–$X^1\Sigma^+$ and $1^1\Pi$–$X^1\Sigma^+$.

The TDMs of the $2^1\Sigma^+$–$X^1\Sigma^+$ and $1^1\Pi$–$X^1\Sigma^+$ transitions are displayed in Fig. 3. It can be seen from Fig. 3 that the TDM for the $2^1\Sigma^+$–$X^1\Sigma^+$ transition reaches a maximum value at $R = 2.11$ Å. However, the TDM for $1^1\Pi$–$X^1\Sigma^+$ decreases with an increase of internuclear distance. At a large internuclear distance approaching the dissociation limit, the TDMs of both $1^1\Pi$–$X^1\Sigma^+$ and $2^1\Sigma^+$–$X^1\Sigma^+$ transitions reach zero. On the basis of our calculated vibrational wavefunctions of low-lying states, we evaluated the FCFs of $1^1\Pi$–$X^1\Sigma^+$ and $2^1\Sigma^+$–$X^1\Sigma^+$ transitions. The FCFs q_{00}, q_{10}, q_{20}, q_{30}, q_{40} and q_{50} of the $1^1\Pi$–$X^1\Sigma^+$ transition are calculated to be 0.08524, 0.19634, 0.23773, 0.20195, 0.13560 and 0.07677, which are in good agreement with experimental values of 0.08131, 0.1944, 0.2417, 0.2081, 0.1390 and 0.07677.[35] The oscillator strength $f_{v'v''}$ is obtained from the FCFs, TDMs and energy gaps of different vibrational levels, which can be used to estimate the band intensity of the spectrum. The oscillator strengths $f_{v'v''}$ of the $1^1\Pi$–$X^1\Sigma^+$ and $2^1\Sigma^+$–$X^1\Sigma^+$ transitions are given in Fig. 4, and the maximum value of $f_{v'v''}$ for the $2^1\Sigma^+$–$X^1\Sigma^+$ transition is twice as large as that for the $1^1\Pi$–$X^1\Sigma^+$ transition. The vibrational band of $1^1\Pi$–$X^1\Sigma^+$ is located in the 35500–38100 cm^{-1} region, with the peak intensity at $v' = 2$. Our simulated result well reproduces the experimental spectrum[35] in the range of 34900–37500 cm^{-1}, with the maximal intensity at $v' = 2$.

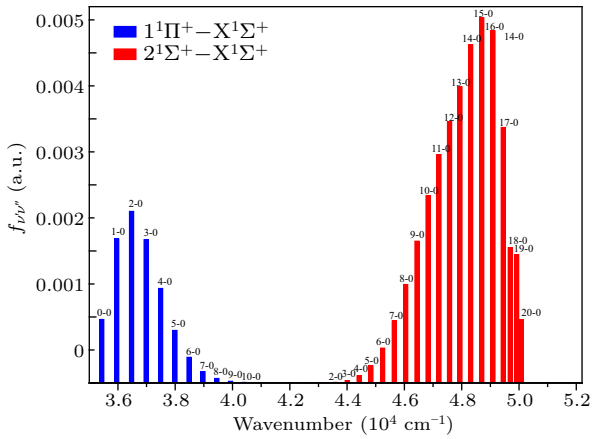


Fig. 4. The calculated oscillator strength of the $1^1\Pi$–$X^1\Sigma^+$ and $2^1\Sigma^+$–$X^1\Sigma^+$ transitions.

3.2. Opacity of the $X^1\Sigma^+$, $1^1\Pi$ and $2^1\Sigma^+$ states of SiS

The opacities of molecules containing sulfur atoms have been extensively studied in the literature by employing the computational approach described in Section 2.[36,37] Molecular opacity is used to determine the species and abundance of elements in fusion physics and astrophysics. Based on the calculated DMs, TDMs, vibration–rotation levels and wavefunctions, the partition function and opacity of the $X^1\Sigma^+$, $1^1\Pi$ and $2^1\Sigma^+$ states of SiS have been calculated. The partition function is a crucial parameter for spectral analysis in astrophysical studies. When dealing with matter in high-density environments, the local thermodynamic equilibrium approximation is used as a practical model, and the molecular opacities are determined by the DMs, TDMs, eigenvalues of vibration–rotation states, degeneracies, and the surrounding temperature

T. The total internal partition function is calculated with formula (7) by considering all of the vibration-rotation levels in the $X^1\Sigma^+$, $1^1\Pi$ and $2^1\Sigma^+$ states. The total internal partition function is computed at different temperatures, and the partition function curves of SiS at different surrounding temperatures are provided in Fig. 5. It can be seen from Fig. 5 that the total internal partition function of SiS exhibits a rapid increase as the temperature T rises. As the temperature increases, the Boltzmann factor $\left(\exp\left(-\frac{T_i hc}{kT}\right)\right)$ exhibits exponential growth, leading to a rapid rise in partition functions determined by formula (7).

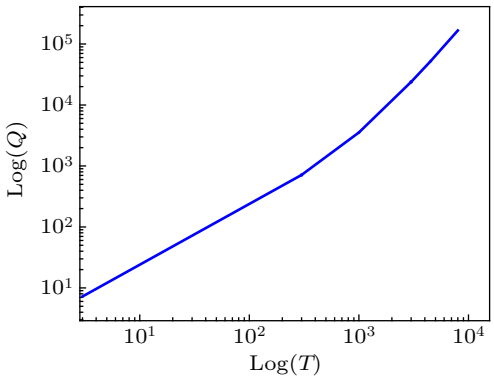


Fig. 5. The variation of partition functions of SiS with the temperature T (in Kelvin).

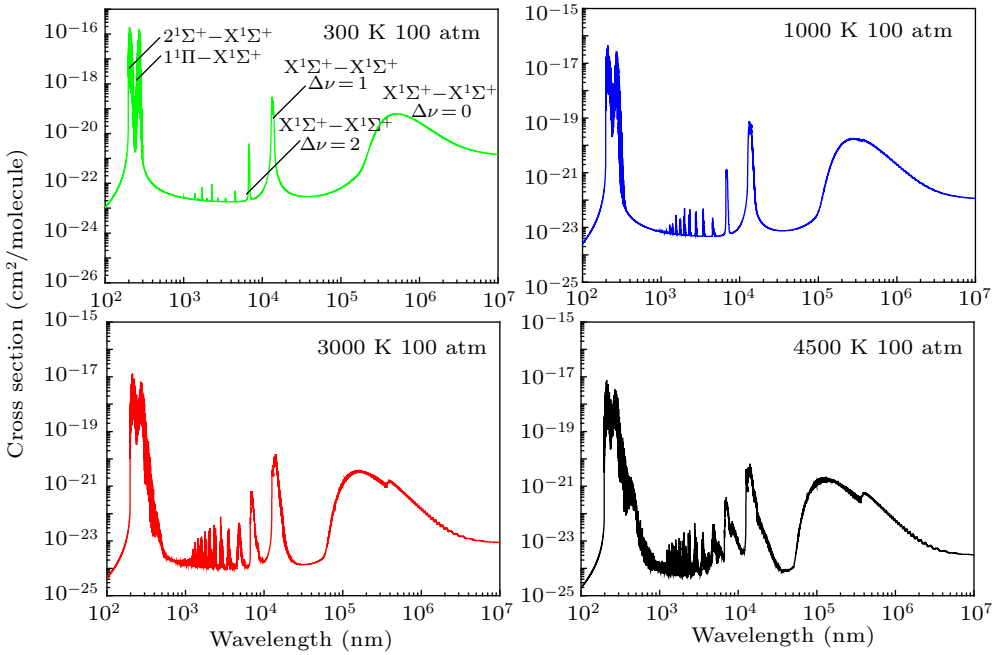


Fig. 6. Opacity of SiS generated by vibration-rotation transitions at a pressure of 100 atms with different temperatures (T = 300 K, 1000 K, 3000 K, and 4500 K).

Based on the calculated partition functions and eigenvalues of vibration–rotation states, the opacities of singlet $X^1\Sigma^+$, $1^1\Pi$ and $2^1\Sigma^+$ states are calculated with formula (6) at a pressure of 100 atms. As discussed in Section 3, the ground state $X^1\Sigma^+$ is a typical bound state, and the dissociation energy of the $X^1\Sigma^+$ is 50828 cm^{-1}; hence, the dissociation probability of SiS induced by thermal motion at a temperature of 4500 K is extremely low. Furthermore, previous work has also indicated that the origin of opacity and the absorption spectrum in astrophysical phenomena predominantly lies within molecular entities.[38,39] In order to illuminate the effect of surrounding temperature on molecular opacities, the molecular opacities originating from the $X^1\Sigma^+$, $1^1\Pi$ and $2^1\Sigma^+$ states of SiS at different surrounding temperatures (300 K, 1000 K, 3000 K and 4500 K) are plotted in Figs. 6(a)–6(d). It can be found from Fig. 6 that the spectra generated by the vibration–rotation transition of the $X^1\Sigma^+$, $1^1\Pi$ and $2^1\Sigma^+$ states of SiS cover a wide wavelength, which is located in the UV to far infrared region. As for the simulated spectra of the $X^1\Sigma^+$, $1^1\Pi$ and $2^1\Sigma^+$ states, the collision-broadened lines are profiled through a Lorentzian function. As shown in Fig. 6(a), there are three bands originating from the $X^1\Sigma^+$, $1^1\Pi$ and $2^1\Sigma^+$ states. These bands correspond to the $2^1\Sigma^+$–$X^1\Sigma^+$, $1^1\Pi$–$X^1\Sigma^+$ and $X^1\Sigma^+$–$X^1\Sigma^+$ transitions, respectively. When the surrounding temperature (300 K and 1000 K) is relatively low, distinct separation between different bands can be observed in Figs. 6(a) and 6(b). The spectral band originating from the $2^1\Sigma^+$–$X^1\Sigma^+$ and $1^1\Pi$–$X^1\Sigma^+$ transitions are located at approximately 210 nm and 261 nm, respectively, falling in the short-wave UV wavelength range. The $X^1\Sigma^+$–$X^1\Sigma^+$ band system exhibits two prominent subbands, which arise from the vibration–rotation transition. The vibrational subbands of $\Delta\nu = 1$ and 2 are centered at wavelengths of 6.7 μm and 13.4 μm, while the pure rotational subband falls within a wavelength coverage of $\geq$ 60 μm. As shown in Fig. 6(a), the absorption spectrum in the range of 350–1300 nm is distinguishable and weak, which

forms an obvious spectral window. As the surrounding temperature increases, the boundary between different bands of electronic transition and fundamental vibrational transitions becomes fuzzy, which is caused by the increased population of electronically excited and vibrationally excited states at higher temperatures. Meanwhile, the cross section attributed to the pure rotational transition ($\Delta v = 0$) evidently reduces due to the significantly decreased populations on the $X^1\Sigma^+$.

4. Conclusions

In this paper, the PECs of 18 Λ–S states of the lowest dissociation limit of the SiS molecule are computed with the MRCI method. Based on the calculated PECs, the vibration–rotation energy levels, wavefunctions and spectroscopic constants are determined using a numerical method. The DMs of the 18 Λ–S states are determined by the MRCI level, and the abrupt change of the DMs for the $1^5\Sigma^+$ and $2^5\Sigma^+$ states around the avoided crossing region are explained by the abrupt variation of configuration. The opacities originating from the singlet states $X^1\Sigma^+$, $1^1\Pi$ and $2^1\Sigma^+$ of SiS are computed at a given pressure of 100 atms with different surrounding temperatures. In lower temperatures (300 K and 1000 K), the spectra originating from the $2^1\Sigma^+$–$X^1\Sigma^+$ and $1^1\Pi$–$X^1\Sigma^+$ transitions are divided into two discrete bands, and the three distinct vibrational bands are attributed to $\Delta v = 0$, 1 and 2 of the $X^1\Sigma^+$–$X^1\Sigma^+$ transition. As temperature increases, the population of excited states increases, leading to the superposition of different transitions. This investigation provides the precise electronic structures, spectroscopic properties and molecular opacities of the excited states of SiS. The work will shed more light on the vibration–rotation spectra and molecular opacity of the SiS molecule.

Acknowledgements

Project supported by the Natural Science Foundation of Heilongjiang Province, China (Grant No. LH2022A026), the National Key Research and Development Program of China (Grant No. 2022YFA1602500), the National Natural Science Foundation of China (Grant No. 11934004), Fundamental Research Funds in Heilongjiang Province Universities, China (Grant No. 145109309), and Foundation of National Key Laboratory of Computational Physics (Grant No. 6142A05QN22006).

References

[1] Upadhyay A, Conway E K, Tennyson J and Yurchenko S N 2018 *Mon. Not. R. Astron. Soc.* **477** 1520
[2] Cami J, Sloan G C, Markwick-Kemper A J, Zijlstra A A, Bauschlicher C W, Matsuura M, Decin L and Hony S 2009 *Astrophys. J.* **690** L122
[3] Sloan G C, Hony S, Smolders K, Decin L, Zijlstra A A, Feast M W, Van Wyk F, Van Loon J Th, Groenewegen M A T and Sahai R 2011 *Astrophys. J.* **729** 121
[4] Danilovich T, Richards A M S, Karakas A I, Van de Sande M, Decin L and De Ceuster F 2019 *Mon. Not. R. Astron. Soc.* **484** 494
[5] Ziurys L M 1991 *Astrophys. J.* **379** 260
[6] Zanchet A, Roncero O, Agúndez M and Cernicharo J 2018 *Astrophys. J.* **862** 38
[7] Barrow R F and Jevons W 1938 *Proc. Math. Phys. Eng. Sci.* **169** 45
[8] Vago E E and Barrow R F 1946 *Proc. Phys. Soc.* **58** 538
[9] Nair K P R, Singh R B and Rai D K 1965 *J. Chem. Phys.* **43** 3570
[10] Gopal S, Lakshminarayana G and Narasimham N A 1980 *J. Phys. B: Atom. Mol. Phys.* **13** 3781
[11] Sunanda K, Gopal S, Shetty B J and Lakshminarayana G 1989 *J. Quant. Spectrosc. Radiat. Transfer.* **42** 631
[12] Prieto L V, Cernicharo J, Quintana-Lacaci G, Agúndez M, Castro-Carrizo A, Fonfría J P, Marcelino N, Zúñiga J, Requena A, Bastida A, Lique F and Guélin M 2015 *Astrophys. J. Lett.* **805** L13
[13] Robbe J M, Lefebvre-Brion H and Gottscho R A 1981 *J. Mol. Spectrosc.* **85** 215
[14] Chattopadhyaya S, Chattopadhyay A and Das K K 2002 *J. Phys. Chem. A* **106** 833
[15] Li R, Zhang X M, Li Q N, Luo W, Jin M X, Xu H F and Yan B 2014 *Acta Phys. Sin.* **63** 113102 (in Chinese)
[16] Fan Q, Tian H, Fan Z, Li H, Fu J, Ma J and Xie F 2023 *Spectrochim. Acta. A: Mol. Biomol. Spectrosc.* **287** 122067
[17] Werner H J, Knowles P J, Knizia G, Manby F R and Schütz M 2012 *Wires. Comput. Mol. Sci.* **2** 242
[18] De Jong W A, Harrison R J and Dixon D A 2001 *J. Chem. Phys.* **114** 48
[19] Peterson K A and Dunning T H 2002 *J. Chem. Phys.* **117** 10548
[20] Werner H J and Knowles P J 1985 *J. Chem. Phys.* **82** 5053
[21] Knowles P J and Werner H J 1985 *Chem. Phys. Lett.* **115** 259
[22] Knowles P J and Werner H J 1988 *Chem. Phys. Lett.* **145** 514
[23] Werner HJ and Knowles P J 1988 *J. Chem. Phys.* **89** 5803
[24] Langhoff S R and Davidson E R 1974 *Int. J. Quantum Chem.* **8** 61
[25] Hess B A 1986 *Phys. Rev. A* **33** 3742
[26] Douglas M and Kroll N M 1974 *Ann. Phys.* **82** 89
[27] Sanz M E, McCarthy M C and Thaddeus P 2003 *J. Chem. Phys.* **119** 11715
[28] Huber K P and Herzberg G 1979 *Molecular Spectra and Molecular Structure IV. Constants of diatomic molecules* (New York: Van Nostrand)
[29] Harris S M, Gottscho R A, Field R W and Barrow R F 1982 *J. Mol. Spectrosc.* **91** 35
[30] Murty A N and Curl Jr R F 1969 *J. Mol. Spectrosc.* **30** 102
[31] Coriani S, Marchesan D, Gauss J, Hättig C, Helgaker T and Jørgensen P 2005 *J. Chem. Phys.* **123** 184107
[32] Green G J and Gole J L 1980 *Chem. Phys.* **46** 67
[33] Coxon J A and Hajigeorgiou P G 1992 *Chem. Phys.* **167** 327
[34] Fan Q C, Tian H R, Fan Z X, Li H D, Fu J, Ma J and Xie F 2023 *Spectrochim. Acta A* **287** 122067
[35] Mummigatti V M and Jyoti B G 1977 *Phys. Lett. A* **63** 88
[36] Li R, Sang J Q, Lin X H, Li J J, Liang G Y and Wu Y 2022 *Chin. Phys. B* **31** 103101
[37] Lin X H, Liang G Y, Wang J G, Peng Y G, Shao B, Li R and Wu Y 2019 *Chin. Phys. B* **28** 053101
[38] Liang G Y, Peng Y G, Li R, Wu Y and Wang J G 2020 *Chin. Phys. Lett.* **37** 123101
[39] Liang G Y, Peng Y G, Li R, Wu Y and Wang J G 2020 *Chin. Phys. B* **29** 023101